Plant Protection (Scientific Journal of Agriculture)
46(3), Autumn, 2023

10.22055/ppr.2024.46044.1733

In silico investigation of pro-peptides from insect zymogens as mimetic inhibitors for digestive chymotrypsin of beet armyworm, *Spodoptera exigua*

S. A. Hemmati [1*], Kh. Pouraghajan [2, 3]

1. ***Corresponding Author:** Associate Professor, Department of Plant Protection, Faculty of Agriculture, Shahid Chamran University of Ahvaz, Ahvaz, Iran (sa.hemmati@scu.ac.ir)
2. Researcher, Department of Science, Vitabiotics Company, Iran Branch, Tehran, Iran
3. Ph.D. Graduate, Bioinformatics Laboratory, Department of Biology, School of Sciences, Razi University, Kermanshah, Iran

Received: 4 February 2024 Accepted: 16 March 2024

Abstract

Spodoptera exigua (Hübner), a highly destructive pest of agricultural crops, is often managed through the use of chemical pesticides. However, the use of chemical pesticides can have negative impacts on human health and the environment, making it important to find sustainable and alternative approaches to effectively manage this pest. One promising solution is the use of inhibitors that hinder the activity of proteases in the insect's digestive tract. Many digestive proteases, such as chymotrypsin, are produced as inactive zymogens with N-terminal pro-regions, which act as intramolecular chaperones and inhibitors of cognate catalytic regions. The present study aimed to utilize various bioinformatics tools to identify the physicochemical properties, secondary structures, and topology of chymotrypsin from *S. exigua*. Furthermore, we evaluated the potential of peptide inhibitors derived from the pro-region of zymogens that could be utilized as mimetic inhibitors for chymotrypsin in *S. exigua*. Homology molecular modeling was performed using SWISS-MODEL, with the predicted model validated by various programs. Molecular docking studies between five homologous species-derived protease inhibitors and the predicted model following by molecular dynamics (MD) simulation coupled with Molecular Mechanics Poisson–Boltzmann Surface Area (MMPBSA) calculations were also applied. The analysis of peptides/enzyme interactions revealed the antagonistic capacity of two screened inhibitors against *S. exigua* chymotrypsin. Protein-protein interaction networks demonstrated that chymotrypsin from *S. exigua* interacted with eleven other proteins in a high confidence score. Active site analysis revealed that S219, D230, and H232 serve as catalytic residues. These findings demonstrate a central role for computational methods in designing a potent inhibitor peptide that is highly specific and selective to its mature enzyme. Our study could be promising for future insecticide designs used in *S. exigua* control.

Keywords: Spodoptera exigua, Chymotrypsin, Pro-peptide, Inhibitory peptide, Pest management

Associate editor: S. Mohammadi (Ph.D.)

Citation: Hemmati, S. A. & Pouraghajan, Kh. (2024). In silico investigation of pro-peptides from insect zymogens as mimetic inhibitors for digestive chymotrypsin of beet armyworm, *Spodoptera exigua*. *Plant Protection (Scientific Journal of Agriculture), 46*(3), 127-142. https://doi.org/ 10.22055/ppr.2024.46044.1733.

Introduction

The beet armyworm, *Spodoptera exigua* (Hübner) (Lepidoptera: Noctuidae), is a polyphagous and detrimental insect pest around the world, which can cause economic damage to various crops, including sugar beet, maize, cotton, soybean and tomato (Smits et al., 1987; Greenberg et al., 2001; Robinson et al. 2010; Fu et al. 2017; Huang et al., 2021). Although chemical pesticides are widely used to control *S. exigua*, their excessive use has resulted in the development of resistance to major classes of insecticides in many regions (Brewer et al., 1990; Wheeler, 2002; Omkar, 2016), leading to the exploration of alternative and safer pest control approaches that are environment-friendly. The development of enzyme inhibitor-based insecticides has introduced a specific and potent class of pesticides for insect pest control (Jitonnom et al., 2012; Hemmati et al., 2021a). Digestive enzymes play vital roles in pests' development and growth by providing essential amino acids (Pereir, 2005; Hemmati et al., 2022). Using inhibitors for the enzymes is a breakthrough in the management of insect pests (Franco et al., 2002). In addition to depleting essential amino acids for pests, inhibiting the digestive enzymes could lead to the hyperproduction of the enzymes which in turn leads to exhaustion of the sulfur amino acids pool, and consequently may cause weakening development and death of the insect pest (Pereir, 2005, Hemmati et al., 2021b). Like the other lepidopterans, the proteolytic enzymes, in particular serine and cysteine proteinases, play a key role in the digestion process of *S. exigua* (Hemmati et al., 2017; Zeng et al., 2019). The digestive enzymes are strictly engaged in the degradation of intra- and extracellular protein, playing crucial roles in the production of free essential amino acids, which are utilized for insect growth (Silva et al., 2007; Hemmati, 2021). Serine proteinases have received particular attention because of their importance in the digestive process of insects. In this regard, using extremely specific and selective pro-regions of proteinases is an intelligent way to inhibit the enzymes (Hemmati et al., 2021b; Jitonnom et al., 2012). Pro-region of a proteinase serves two crucial functions: 1) it guides the proper folding of the mature enzyme, and 2) it acts as an inhibitor of proteolytic activity by blocking the enzyme from accessing the substrate (Baker et al., 1993; Hemmati et al., 2021b). Consequently, the pro-regions could be potent inhibitors for the digestive enzyme and hence be promising in pest control.

It has been documented that the synthetic peptides, identical to the pro-region of the *Manduca sexta* (L.) midgut trypsin, can inhibit the mature enzyme (Taylor & Lee, 1997). Moreover, recombinantly expressed pro-region in papaya proteinase IV has been reported to inhibit *Leptinotarsa decemlineata* Say digestive cysteine proteinases activity (Visal et al., 1998). Jitonnom et al. designed a peptide inhibitor for *Plutella xylostella* (L.) midgut trypsin through modification in the pro-region of the pest trypsinogen structure (Jitonnom et al., 2012). Furthermore, it has been shown that the pro-peptide region was capable of inhibiting the cysteine protease of *Acanthoscelides obtectus* (Say) without any inhibitory effect on other species of the coleopterans (Silva et al., 2007). Investigating the potential of the pro-region as an inhibitor of chymotrypsin in *Helicoverpa armigera* (Hübner) revealed that the inhibitor exhibited the most favorable binding affinity for interactions with the chymotrypsin's active site of the pest. However, it exhibited weak potential to bind the porcine (*Sus scrofa* L.) chymotrypsin (Hemmati & Karam Kiani, 2021). Hemmati et al. (2021b) designed several inhibitor peptides based on the zymogen structure of *Plodia interpunctella* (Hübner) trypsin and the findings suggested that an inhibitor peptide could effectively and specifically inhibit the pest midgut trypsin and has no effect on porcine trypsin as a model of the mammalian enzyme (Hemmati et al., 2021b).

In the present work, we have designed five inhibitor peptides based on pro-region of

homologs sequences, and their binding affinities toward the chymotrypsin from *S. exigua* have been characterized using molecular docking and molecular docking (MD) simulations coupled Molecular Mechanics Poisson–Boltzmann Surface Area (MMPBSA) calculations. Structural and physiochemical properties, as well as the protein-protein network interaction of the chymotrypsin from *S. exigua* were also assessed. Here, *in silico* studies can help us understand some structural and binding features of the inhibitor peptides toward the target enzyme, mainly their binding affinities to the active site of the enzyme. The best-scoring designed inhibitor peptide can be selected for further screening using *in vitro* and *in vivo* analysis. Our results propose that this inhibitory peptide could serve not only as a next-generation insecticide but also as a new biotechnological tool to generate genetically modified pest-protected plants.

Materials and Methods

Sequence analysis and homologous sequence searching

The amino acid sequences of midgut chymotrypsin of *S. exigua* (Q3ZJD2) were retrieved from UniProt (https://www.uniprot.org/uniprotkb/Q3ZJD2/). Homologous sequence searching was performed using the sequence search tool, BLASTP on NCBI. Sequences were derived from the EMBL/Gen-Bank database for multiple sequence alignment using Clustal Omega-Multiple Sequence Alignment (https://www.ebi.ac.uk/Tools/msa/clustalo/). Selected pro-peptide sequences were subjected to Hyperchem software (version 8.0, HyperChem Professional Inc) based on the energy minimization using the Fletcher-Reeves algorithm program, while N- and C-terminals were checked for the correct charges.

S. exigua midgut chymotrypsin 3D modeling, analysis, validation, and active site identification

A 3D structure of the protein was modeled by comparative protein modeling methods using the SWISS-MODEL server (http://swissmodel.expasy.org). A suitable template for homology modeling was selected using the SWISS-MODEL template searching method in AlphaFold Data Base. The model coordinates were improved by removing spatial restraints by using the ModRefiner method in Zhang Lab (https://zhanggroup.org/ModRefiner/), which poses an atomic-level energy minimization-based algorithm. To analyze the structural evaluation and stereochemical quality and accuracy assessment of the predicted models, ProQ (https://proq.bioinfo.se/cgi-bin/ProQ/ProQ.cgi), ProSA (https://www.came.sbg.ac.at/prosa.php), ERRAT, VERIFY 3D, and PROCHECK which are available online at the UCLA-DOE Lab-SAVES v6.0 server (https://saves.mbi.ucla.edu/) were used. The computed Atlas of Surface Topography of proteins (CASTp) webserver was used to identify geometric and topological properties of the protein structure to find out the binding site properties and active site catalytic residues (http://sts.bioe.uic.edu/castp/calculation.html). Expasy ProtParam was applied to characterize the physicochemical properties of the *S. exigua* midgut chymotrypsin, including molecular weight, theoretical pI (isoelectric point), instability index, and aliphatic index (https://web.expasy.org/protparam/). The secondary structure composition was predicted in SOPMA (self-optimized prediction method with alignment) (http://npsa-pbil.ibcp.fr/cgi- bin/). Identification of protein-protein interaction was carried out by STRING web tool (https://string-db.org/), which is a biological database used to construct protein-protein interaction networks for different known and predicted protein interactions.

Prediction of affinity binding energy by HEX program docking and dissociation constant

The HEX docking procedure was used to examine the binding affinity and molecular interactions between peptides and *S. exigua* chymotrypsin (Macindoe et al., 2010). First, the polar hydrogen atoms were added to the coordinates of the receptor. The energy of the interaction was calculated based on shape,

electrostatic, and DARS (Decoys As the Reference State) energies as correlation type; docking Fast Fourier Transform (FFT) devices were set on the CPU; maximum docking cluster members and maximum docking clustering window were 500 and 200, respectively. Docking was performed using the main scan on 18 and a final search on 25, while 500-docked structures were generated for each run. The other parameters were set to default. Additionally, the PRODIGY (protein binding energy prediction) webserver available at (https://bianca.science.uu.nl/prodigy/) was applied to calculate the binding energy (ΔG) and dissociation constant (*Kd*) at 25°C. This webserver predicts binding affinities based on inter-molecular contacts within a distance cut-off of 5.5 Å.

Molecular dynamics simulations and binding free energy calculations

The molecular dynamics (MD) simulation experiment was performed using the GROMACS simulation package with the gromos 54a7 force field (Van Der Spoel et al., 2005). The MD simulation for evaluation of the molecular behaviors and particularly for the preparation of the initial-to-final coordinated for the following Molecular Mechanics Poisson–Boltzmann Surface Area (MM/PBSA) calculations via the GROMACS implemented g-mmpbsa program. The protein/peptide complex was first located in the center of the cubic box by randomly adding the water molecules in the SPC/E model as the solvent and NaCl in a 0.2 M concentration to neutralize and buffer the system. As the pH can affect the protonation states of amino acids and other chemical species, which in turn can influence the structure and dynamics of the system, the *S. exigua* is characterized by a very alkaline gut environment (pH > 9.0), the pH of the simulation directly set on 10 using the appropriate protonation states for the ionizable groups. Prior to the simulation, the system was subjected to 50,000 steps of steepest descent energy minimization and system equilibration under the NVT ensemble in 500 ps. The temperature was set at 300 ^{o}K using the Berendsen algorithm with a time constant of 0.1 ps. The next equilibration phase was performed for 500 ps under the NpT ensemble, where the pressure was controlled at 1 bar using the Parrinello–Rahman algorithm and a pressure coupling time constant of 0.2 ps. The linear constraint solver (LINCS) algorithm was used to constrain all bonds. A periodic boundary condition (PBC) was applied in the x-, y-, and z-directions. The short-range Van der Waals interactions in the Lennard–Jones (LJ) potentials were cut off at 1.4 nm. A particle-mesh Ewald (PME) algorithm was applied to deal with the long-range electrostatic interaction of Coulomb potential energies with the real-space contribution to the Columbic interactions truncated at 0.9 nm. The initial velocity of the particles was generated according to Maxwell distributions to produce a 50 ns MD simulation by saving coordinates in time intervals of 10 ps. Trajectory snapshots were taken for structural analysis, including Root Mean Square Deviation (RMSD) and radius of gyration (Rg), through gross utilities. All indicator analyses were performed in the thermodynamically stable state of the simulation trajectory, where the system RMSD graph reached a plateau. The interaction analysis of the peptides/enzyme was performed using LigPlot^{+} and Discovery Studio. Computational alanine scanning for peptides hot spot finding done using the DUBE Alanine Scan web tool (https://pragmaticproteindesign.bio.ed.ac.uk/balas/). All schematic graphic representations were generated using the UCSF Chimera package.

Results and Discussion

***In silico* homology modeling**

De novo homology-based molecular modeling of the *S. exigua* chymotrypsin was performed using the SWISS-MODEL template searching method in AlphaFold Data Base. The model generated with A0A2H1X2T2-SPOFR originated from *Spodoptera frugiperda* (J.E.Smith) as the template with a sequence identity of 80.5% and global model quality estimation (GMQE) score of 0.93 (Figure 1A).

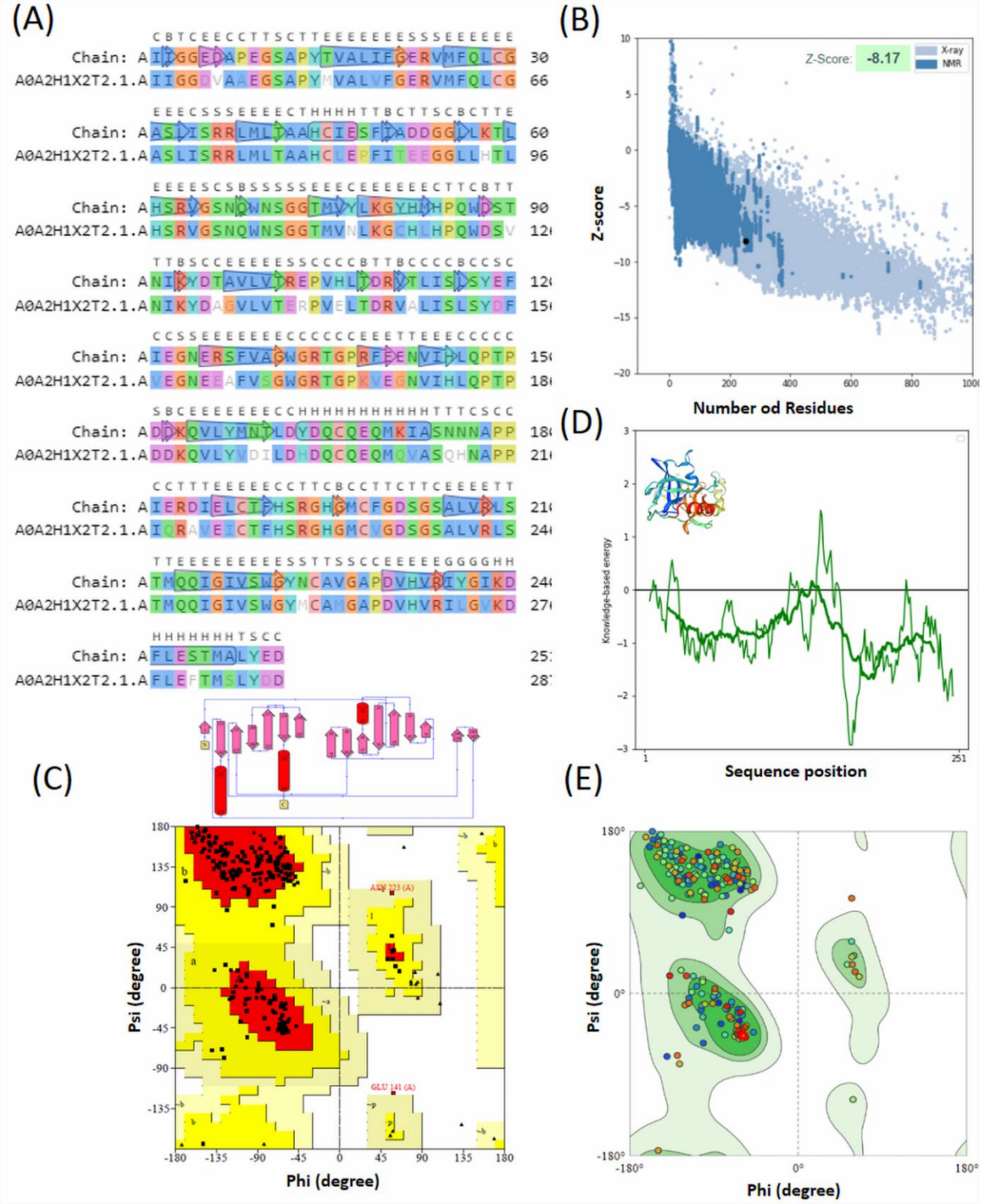

Figure 1. Model structure validation (A) chymotrypsin and SWISS-Model AlphaFold DB template alignment with 80.5% sequence identity, (B) ProSA web server results presented with the Z-scores (black dot) and (D) energy plots which illustrated the local model quality. ProSA-web Z-scores fall in defined protein chains in RCSB PDB determined by X-ray crystallography (light blue) and NMR spectroscopy (dark blue), Ramachandran plots generated via (C) secondary structure elements, PROCHECK, and (E) SWISS-Model, both predicted that the residues in most favored (red in PROCHECK and dark green in SWISS-Model), additionally allowed (yellow in PROCHECK and light green in SWISS-Model), generously allowed (pale yellow in PROCHECK and pale green in SWISS-Model) and disallowed regions (white color).

Also, the predicted LG score in ProQ (>4, extremely good model) and MaxSub score (>0.8, extremely good model) was within an acceptable range as follows: LG score, 6.733; MaxSub, −0.342. The quality of the dimensional coordinates is a given ProSA Z-score, which describes the potential errors or the deviation of the total energy of the structure concerning the energy distribution profile of the experimentally known structures with X-ray or NMR. The predicted model ProSA Z-Score was −8.17, indicating no significant deviation from typical native structures (Figure 1B). The folding energy of the model in terms of the energy function of amino acid residues was also analyzed with ProSA. The energy plot revealed a minimum value as this accounts for the stability and nativity of the molecules, consistent with a reliable conformation (Figure 1D). The stereochemical evaluation of the model geometry was also performed using Ramachandran's plot calculations in PROCHECK and SWISS-MODEL (Figure 1C, E).

The computed backbone Psi and Phi dihedral angles of the model revealed that most residues fell within the favored regions, which are depicted in Table 1. In general, from PROCHECK results, the predicted model gained accepted stereochemical quality scores. Other analyses found no bad contacts or bad scores for main chain or side chain parameters. The G-factor demonstrates how unusual a stereochemical function is. The overall G-factor values (Goodness factor) of the model were acceptable values of the G-factor in PROCHECK (between 0 and −0.5, with the best-quality models displaying values close to zero) (Table 1). Afterwards, for a more confident model, ERRAT structure verification was performed. ERRAT works according to the analysis of the statistics of non-bonded interactions between different atom types; higher scores indicate higher quality. The ERRAT overall quality factor was 97.5, while the generally accepted range was >50 for a high-quality model according to the underlying basic algorithm (Table 1), which is well suited for evaluating the quality of crystallographic model building and refinement. The model was then verified by VERIFY 3D, which presented that 89.7% of residues of the model had an average 3D-1D score greater than 0.2. Verify3D analyzed the compatibility of the 3D (atomic coordinates) model with its amino acid sequence (1D).

S. exigua Chymotrypsin active site identification

For the next level of docking experiment, we analyzed *S. exigua* chymotrypsin's active site as a digestive serine protease enzyme. The general action mechanism of chymotrypsin includes an active serine, aspartic acid, and histidine residues called an active site triad. The catalytic triad is located in a hydrophobic binding pocket to perform hydrolysis on the substrate C-terminus of the aromatic amino acids (F, W, and Y residues). Chymotrypsin kinetics comprises two phases: pre-steady-state and steady-state through the "Ping-Pong" mechanism, the formation of covalent complexes leading to covalent hydrolysis reactions, and the rate of the catalyzed reactions. Upon the target enters the active site of chymotrypsin, it is held there by hydrophobic interactions between exposed non-polar groups of enzyme residues and the non-polar aromatic side-chain of the substrate. Here, the hydrogen bond between the Schiff nitrogen on histidine and the oxygen side-chain of serine is important for intermediate fixing to be ready for the hydroxyl group on serine nucleophilic attack on the carbonyl carbon of an aromatic amino acid.

Table 1. Validation of chymotrypsin structure backbone psi and Phi dihedral angles using PROCHECK and ERRAT score.

Ramachandran plot statistics (%)				Goodness factor*			ERRAT
Most Favored	Additionally Allowed	Generously Allowed	Disallowed	Dihedral Angles	Covalent Forces	Overall Average	Score
89.8	9.3	0.5	0.5	−0.09	−0.13	−0.06	97.5

*Lower than −0.5, unusual; lower than −1.0, highly unusual.

Simultaneously, the hydrogen bond between the histidine nitrogen and aspartic acid carboxyl oxygen is needed for catalysis. Therefore, according to the general catalytic mechanism of chymotrypsin, S, D, and H residues are needed to perform hydrolysis. The surface area, the volume of the active site pocket, and the residues forming the pocket were obtained using CASTp 3.0 sequence analysis and visual inspection of the residues and distance measurements. All the S, D, and H residues in the predicted pocket were visually inspected, and S219, D231, and H232 were spatially distributed in the accepted distance to be susceptible to the catalytic triad (Figure 2). Totally, from 40 identified pockets, the catalytic site cleft corresponded to one pocket with (Area: 81.475 Å2, Volume: 20.950 Å3) properties, and the involved amino acids in creating binding pockets included L156, M158, F190, H191, S192, H195, G196, M197, C198, F199, D201, S202, V218, S219, W220, G221, Y222, N223, 224, A225, V226, G227, A228, P229, D230, V231, H232 (Figure 2).

Secondary structure and physicochemical properties of the *S. exigua* chymotrypsin

The Expasy's ProtParam and SOPMA web tools results are summarized in Table 2. Secondary structure analysis by SOPMA revealed that the structure elements were composed of random coils (24.7%), α-helices (7.9%), β-strands (43.9%), and β-turns (23.5%). Therefore, the predominant structural elements present in the enzyme were β-strands. Also, the content of the secondary structures from the amino acid sequence was compared with the content of the secondary structures in the modeled three-dimensional structure. The results in both cases were consistent with slight differences. The secondary structure topology displaying 3 helices (H1-H3) is involved in 1 helix-helix interactions, while 3 β-sheet motifs composed of 16 β-strands, 8 β-hairpins, 6 β-bulges, 31 β-turns, 2 γ-turns, and 3 disulfide bonds (Fig. 1). The computed pI value was 5.20, indicating the overall acidic character of the enzyme.

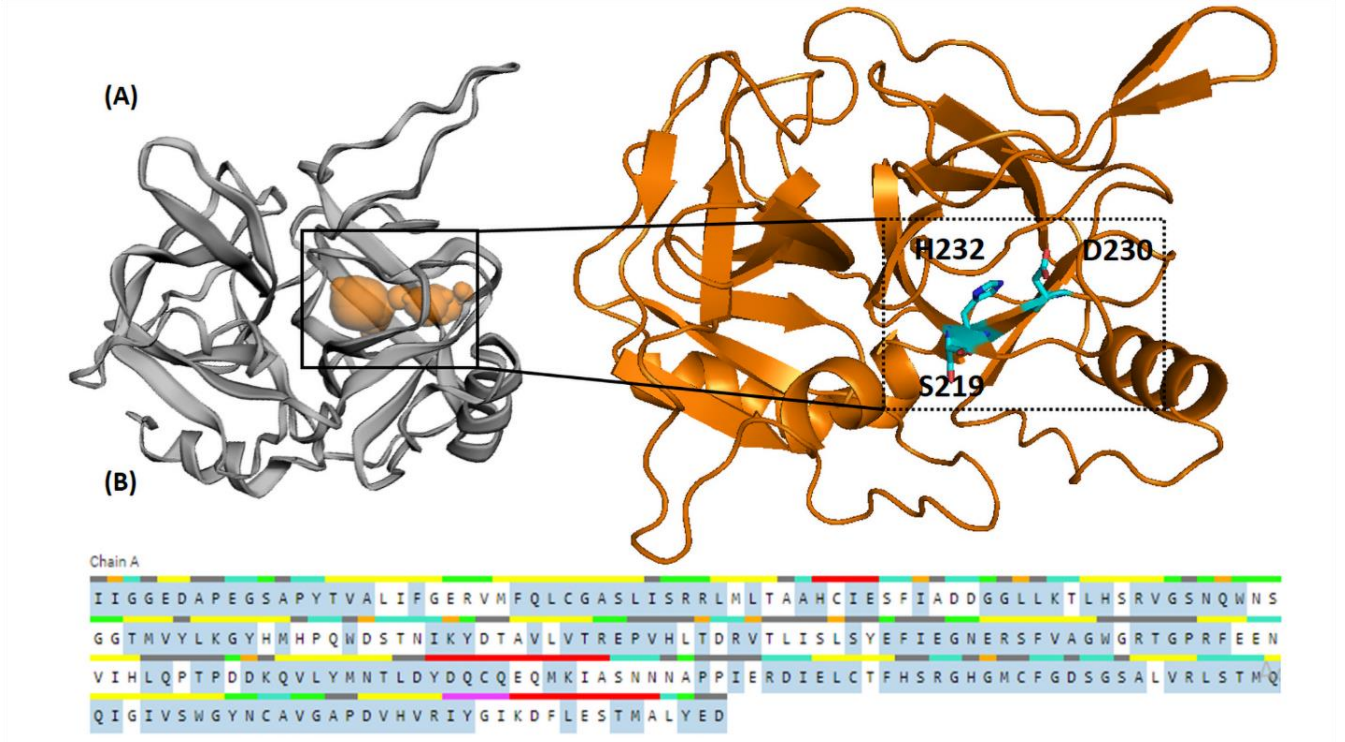

Figure 2. CASTp webserver geometric and topological analysis of the chymotrypsin binding site and catalytic residues. Enzyme presented as ribbon gray and orange structure. (A) Projection of the predicted active site. Three obtained binding cavities colored brown. Catalytic triad colored as blue licorice structures. (B) CASTp webserver sequence analysis.

Table 2. *In silico* predictions of physicochemical properties, secondary structures, and topology in Expasy's ProtParam and SOPMA web tools for chymotrypsin.

Tools	Parameter		Value
ProtParam	Number of amino acids (AA)		251
	Molecular weight (Mw)		27957.65
	Theoretical isoelectric point (pI)		5.20
	Instability index		38.43
	Aliphatic index		83.51
	GRAVY index		-0.178
SOPMA	α-Helix (%)	Sequence	7.9
		3D Model	9.2
	β-Strand (%)	Sequence	43.9
		3D Model	41.4
	β-Turn (%)	Sequence	23.5
		3D Model	21.5
	Random Coil (%)	Sequence	24.7
		3D Model	27.9

According to the instability index computed using Expasy's ProtParam server, 38.43, the enzyme was classified as stable (instability index < 40). The increase in the aliphatic index is defined as the relative volume of a protein occupied by an aliphatic side chain, which increases the thermostability of globular proteins. The calculated index was 83.51 which indicates that the protein is stable and active over a wide range of temperatures. The very low grand average of hydropathicity (GRAVY) index (−0.178) suggested that the protein could interact with water in solution (hydrophilic in nature), suggesting the localization of this protein in the cytoplasm or nucleus.

Peptide library preparation

Pro-regions in protease enzymes are naturally considered potent and specific inhibitors of their associated proteases. Here, we assigned the sequences of pro-peptides from homologous sequences with sequence identity scores above 80%. The *S. exigua* chymotrypsin was extracted from UniProt and then subjected to homologous sequences searching via the NCBI protein blast tool. Then, the amino acid sequences with sequence identity above 80% including chymotrypsin [*Spodoptera exigua*] (GenBank accession number: AAX35812.1), hypothetical protein HF086_018183 [*Spodoptera exigua*] (GenBank accession number: KAH9639115.1), unnamed protein product [*Spodoptera littoralis*] (GenBank accession number: CAB3507546.1), chymotrypsin-1-like [*Spodoptera frugiperda*] (GenBank accession number: XP_050550258.1), hypothetical protein SFRURICE_013210 [*Spodoptera frugiperda*] (GenBank accession number: KAF9801430.1), serine protease, partial [*Clostridium perfringens*] (GenBank accession number: MDK0809123.1), and hypothetical protein B5X24_HaOG200518 [*Helicoverpa armigera*] (GenBank accession number: PZC74509.1) were aligned for pro-peptide region extraction. Finally, five propeptide sequences including **VPLPSDPKPF**, **VPLPSSDHQAF**, **VPLPSSDHEVF**, **VPLPPSDHQPF**, and **VPLSPSDHQPF** were selected.

Molecular docking study

Prediction of affinity binding energies and the best-docked pose for peptides/enzyme complexes were performed in the HEX program, which uses fast Fourier transform (FFT)-based protein blind docking. It uses cartesian grid–based FFT docking algorithms for the spherical polar Fourier (SPF) approach, which is repeated over multiple rotational samples to cover the 6D search space with rotational correlations. Afterwards, the best enzyme/peptide complexes were screened according to the best energies and lowest distance between the enzyme active site catalytic triad. Peptide-3 was not placed in the active site cavity in blind docking experiments, and as such it was neglected in the next analysis. The selected

complexes belonged to HEX's E_{Total} values in this range; peptide-1/enzyme: −476.4 kJ/mol, peptide-2/enzyme: −472.9 kJ/mol, peptide-4/enzyme: −453.0 kJ/mol, and peptide-5/enzyme: −459.9 kJ/mol. The negative and low value of E_{Total} indicated a stronger affinity between enzyme and peptide related to native peptide-1/enzyme as the standard reference. Therefore, the selected four complexes were subjected to the next assessment level in MD simulations.

MD simulation and evaluation of peptide/enzyme complexes interactions

In the present research, four 50 ns MD simulations were run with peptide-1, peptide-2, peptide-4, and peptide-5/enzyme complexes. By visual inspection of the extracted coordinates along the simulation trajectory, we observed that peptide-2/ and peptide-4/chymotrypsin complexes dissociated after about 15 and 10 ns from the initial step of the simulation respectively, and were excluded from the next levels of evaluations. Figure 3C revealed the RMSD values of all complex structures over the simulation trajectory. The calculated RMSD values in graphs for peptide-1/chymotrypsin and peptide-5/chymotrypsin complex structures were less deviated and reached a thermodynamically stable state after 10 ns. For peptide-2/ and peptide-4/chymotrypsin complexes RMSD values showed high fluctuation structures. From RMSD results, it can be concluded that the peptide-1/chymotrypsin and peptide-5/chymotrypsin complexes were more stable than the other complex structures with peptides less ΔRMSD before and after simulation (Peptide-1 ΔRMSD: 0.65 nm, Peptide-5 ΔRMSD: 0.54 nm, (Figure 3A, B)). These results were consistent with PROGIGY higher calculated *Kd* values for peptide-2/and peptide-4/chymotrypsin complexes (Table 3). For all four systems, the protein RMSD fluctuates in these ranges; peptide-1/enzyme: 0.12−0.17 nm, peptide-2/enzyme: 0.11−0.2 nm, peptide-4/enzyme: 0.12−0.25, and peptide-5/enzyme: 0.12−0.21nm, suggesting the overall stability of the protein during the 50 ns MD simulation for all systems but the more range of fluctuations for chymotrypsin in complex with peptide-2 and peptide-4 subjected for more structural evaluations.

Given these, the Rg analysis performed which is an indicator for the distribution of atoms of a protein around its axis and is a measure of the compactness of the protein. The enzyme Rg in the peptide-1/chymotrypsin and peptide-5/chymotrypsin in the systems was found to range between 1.28 to 1.32 nm, and 1.29 to 1.32 nm, respectively (Figure 3D). Indeed, these values show a higher increase the overall compactness of the peptide-2/ in chymotrypsin and peptide-4/chymotrypsin after dissociation from peptides to lose their intact structures and compactness with volatile Rg values ranging from 1.28 to 1.35 nm for peptide-2/chymotrypsin and 1.29 to 1.35 nm for peptide-4/chymotrypsin. In conclusion, structural indicator analysis from MD simulations revealed that the interactions of peptide-1 and peptide-5 were suitable enough. These results for peptide-1/chymotrypsin and peptide-5/chymotrypsin complex existence along the simulation time demonstrated that the binding energy and the binding pattern could be adequate to reach the inhibition phenomenon as it had been proven more in the following MMPBSA total binding free energy ($\Delta G_{Binding}$) analysis.

The $\Delta G_{Binding}$ and based on the underlying theory of the method, the polar and nonpolar parts of this value were estimated using MMPBSA computations. The procedure is path-independent and calculated energy functions on an ensemble of extracted coordinates in each state of MD simulation performed using the g-mmpbsa program (Kumari et al., 2014). The calculation was performed after 10 ns for peptide-1/chymotrypsin and peptide-5/chymotrypsin complexes where the system RMSD reached a thermodynamically stable state (Figure 3C) and for peptide-2/chymotrypsin and peptide-4/chymotrypsin before chymotrypsin dissociation from peptides. Because convergence to equilibrium is a necessary condition for molecular simulation and interaction study. According to MMPBSA results (Table 3), the total binding free energy (ΔGBinding) for complexes was estimated

as peptide-1/chymotrypsin: −215.1 ± 14.1 kJ/mol, and peptide-2/chymotrypsin: −202.1 ± 8.1 kJ/mol, peptide-4/chymotrypsin: −179.2 ± 18.2 kJ/mol, and peptide-5/chymotrypsin: −222.7 ± 16.4 kJ/mol, respectively. These values were further divided into the nonpolar ($\Delta G_{Nonpolar}$) (the contribution of the Van der Waals interactions plus nonpolar solvation-free energy) and polar (ΔG_{Polar}) parts (composition of electrostatic interactions plus polar solvation energy). As depicted in the results suggest that nonpolar interactions play a major role in the stabilization and probably the driving forces forming the complexes.

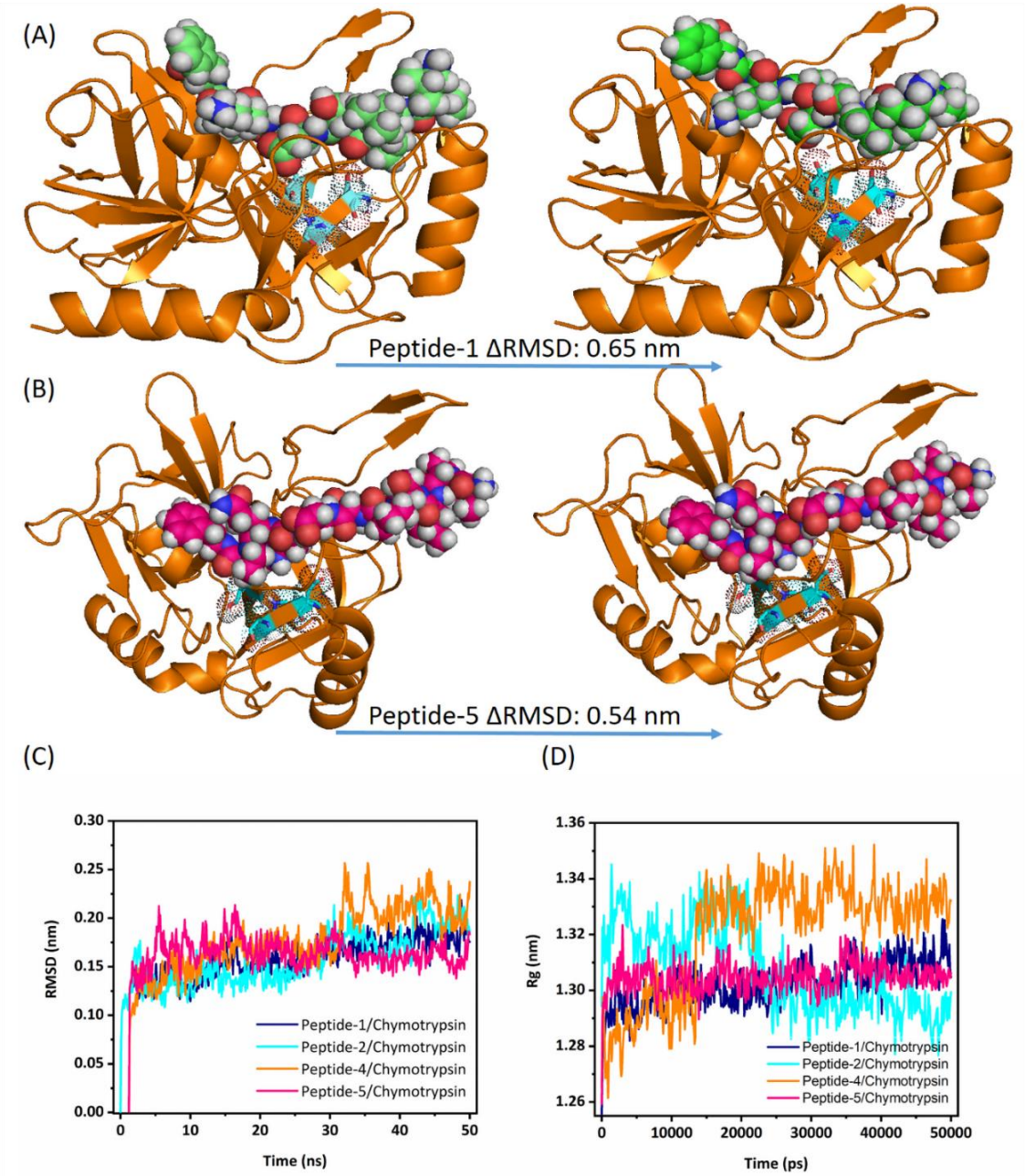

Figure 3. The structure of the (A) peptide-2/enzyme and (B) peptide-5/enzyme complexes after HEX docking (left site) and the predominant snapshot of the MD simulation (right site). The enzyme is colored orange ribbon, and the catalytic triad is colored cyan dot licorice. MD simulation changes upon mutations. (C) Root mean square deviations (RMSD) and (D) Radius of gyration (Rg) of the complexes.

Table 3. HEX molecular docking affinity energy, MMPBSA, and PRODIGY computations results.

Pro-peptide	Sequence	GenBank AcN	HEX E_{Total} (kJ/mol)	MMPBSA (kJ/mol)			PRODIGY (kcal mol^{-1})	
				$\Delta G_{Binding}$	$\Delta G_{Nonpolar}$	ΔG_{Polar}	ΔG	K_d (M)
Peptide-1	VPLPSDPKPF	AAX35812.1	−476.4	−215.1 ± 14.1	−162.0 ± 10.3	−53.1 ± 6.1	-11.1	7.8e-09
Peptide-2	VPLPSSDHQAF	CAB3507546.1	−472.9	−202.1 ± 8.1	−144.2 ± 20.3	−57.9 ± 11.9	-12.0	1.6e-09
Peptide-3	VPLPSSDHEVF	XP_050550258.1	-	-	-	-	-	-
Peptide-4	VPLPPSDHQPF	KAF9801430.1 PZC74509.1	−453.0	−179.2 ± 18.2	−106.4 ± 8.3	−72.8 ± 19.2	-10.8	1.1e-08
Peptide-5	VPLSPSDHQPF	MDK0809123.1	−459.0	−222.7 ± 16.4	−185.7 ± 20.1	−37.0 ± 12.4	-11.5	3.9e-09

Peptide-1 and peptide-5 interaction analysis and hot spot finding

Post-MD results illustrated that peptide-1 and peptide-5 conserved their interaction pose along the trajectory. The results were shown in Figure 4 (expanded) which revealed an efficient potent interaction with the active site S219 and H232 residues. A more detailed investigation revealed strong H-bond interactions among residues within the active site for both peptides (Figure 4). Peptide-1 along with S291 and H232, and peptide-5 with S291 were in hydrogen interactions. Additionally, the Van der Waals forces presentation suggested the possibility that peptides have hot spot species responsible for interaction with enzyme as indicated above. This may ultimately lead to inhibition of *S. exigua* chymotrypsin activity in the catalytic site composed of crucial catalytic residues S219, H232, and D230. However, further biochemical wet lab experiments would be necessary to provide more convincing evidence for the above hypothesis. Based on these interaction maps the binding interaction's most favorable residues were extracted in the hot spot finding procedure. The energy distribution along the protein–peptide interface is not homogenous; certain residues contribute more to the binding free energy, called hot spots are the most important residues and binding driving favoring forces. In protein engineering, alanine-scanning mutagenesis involves the replacement of the residues with alanine to determine the energetic contribution of each side chain to forming an interaction. The differences in binding energies in two modes, including residue in native wild-type and residue mutation to alanine amino acid ($\Delta\Delta G = \Delta G_{wild\text{-}type} - \Delta G_{Ala\text{-}mutation}$), obtained from the computational alanine-scanning mutagenesis. Negative $\Delta\Delta G$ values indicate unfavorable substitution for alanine in the relevant position and reveal the importance of the mutated residue in the binding phenomenon. The *in silico* hot spot finding through alanine scanning depicted in Table 4 presented that for peptide-1, V1, P2, D6, and P7, and peptide-5, S4 and P9 are the most critical residues for binding (Table 4).

Further deep analysis through visual inspection with cognizing on chymotrypsin action mechanism for each residue function presented the peptide-1 P2, D6, and P7 as the most important hot spots. Furthermore, since no effective interaction with enzyme catalytic triad was found for peptide-1 V1 residue, it was clear that peptide-1 V1 residue negative $\Delta\Delta G$ value in hot spot finding calculations was related to interaction with water for solubility and stabilizing the interaction. In addition, the P2 residue in peptide-1 has the highest negative $\Delta\Delta G$ values, which was related to the deep hydrophobic burial of this residue at the recognition site and anchoring it to the protein for maintaining binding strength (Figure 5A). Finally, D6 and P7 interface with the stabilizing hydrogen bonding pattern between chymotrypsin S219 and H232 catalytic residues (Figure 5A). Peptide-1 D6 and P7 make hydrogen bonds with chymotrypsin H232 and S219, respectively, to disrupt the hydrogen bond between S219 and H232, which is needed for the catalysis function of the enzyme (Figure 5A). In the case of the peptide-5, from $\Delta\Delta G$

values and visual inspections, S4 and Q9 via Van der Waals interactions and S6 through hydrogen bonding with chymotrypsin C224 and C198 acts as the anchoring and recognition residues for peptide-5 binding. Peptide-5 H8 makes a hydrogen bond with chymotrypsin S219 and breaks the stabilizing hydrogen bond between S219 and H232 (Figure 5B).

The protein-protein interacting partners of chymotrypsin from *S. exigua*

For more characterization of the *S. exigua* midgut chymotrypsin properties, the enzyme interacting partners network was generated through STRING 12.0 (Figure 6). The STRING database analysis illustrated that *S. exigua* chymotrypsin network comprised 11 nodes connected with 40 different edges with enrichment p-value: 6.36e-10. While the expected number of edges was observed to be 13; the average node degree score was found to be 7.27. STRING forecasted confidence scores representing the functional network among the set of proteins of a given organism were between 0.66–0.99.

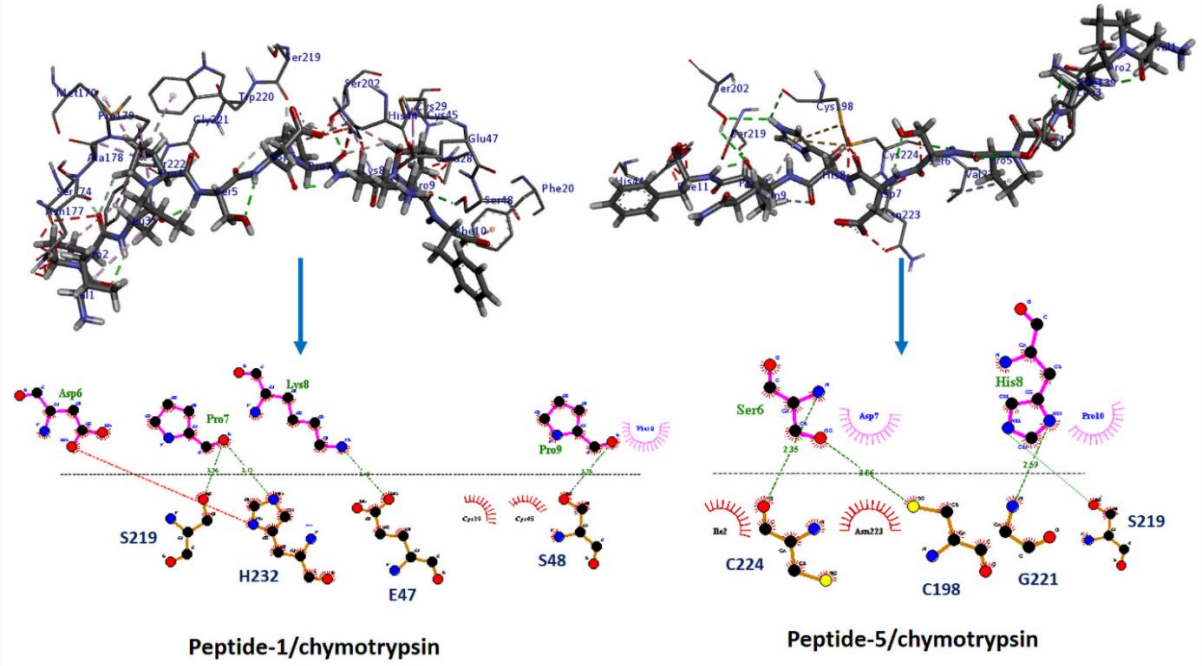

Figure 4. Peptide-1/ and peptide-5/chymotrypsin interacting amino acids.

Table 4. Alanine scanning mutagenesis results for peptide-1 and peptide-5 hot spots in chymotrypsin binding using the DUBE Alanine Scan web tool.

Peptide-1 Amino Acid	Total ΔG: −18.57 ΔΔG (kJ/mol)	Peptide-5 Amino Acid	Total ΔG: −23.43 ΔΔG (kJ/mol)
V1	**−4.40**	V1	0.1
P2	**−65.80**	P2	1.6
L3	6.20	L3	3
P4	−0.02	**S4**	**−22.9**
S5	3.40	P5	3.2
D6	**-37.15**	**S6**	**-15.6**
P7	**−2.80**	D7	−0.2
K8	8.10	**H8**	**-9.9**
P9	0.50	**Q9**	**−11.6**
F10	3.40	P10	4.5
-	-	F11	11.2

S. exigua chymotrypsin was predicted to be interacting with 10 proteins, namely clpX, EEZ60421.1, clpB, tig, dnaK, grpB, groS, groL, hrcA, and def in different functions from *S. exigua*. ClpX is an ATP-dependent protease. EEZ60421.1 is an ATP-dependent protease associated with various cellular activities as a part of the multi-chaperone system with dnaK, dnaJ. ClpB is an ATP-dependent chaperone protein; part of a stress-induced multi-chaperone system involved in the recovery of the cell from heat-induced damage in cooperation with dnaK, dnaJ, and grpE. Tig is a trigger factor involved in protein export. It acts as a chaperone by maintaining the newly synthesized protein in an open conformation. It functions as a peptidyl-prolyl cis-trans isomerase. Dnak is a chaperone protein belonging to the heat shock protein 70 family. GrpE is a Co-chaperone thermosensor that participates actively in the response to hyperosmotic and heat shock by preventing the aggregation of stress-denatured proteins in association with dnaK. GroS and groL are chaperones and prevent misfolding and promote the refolding and proper assembly of unfolded polypeptides generated under stress conditions. HrcA is a heat-inducible transcription repressor, a negative regulator of class I heat shock genes (grpE-dnaK- dnaJ and groELS operons). It prevents heat-shock induction of these operons. Finally, def is a peptide deformylase and removes the formyl group from the N-terminal Met residue of newly synthesized proteins. Therefore, the S. *exigua* chymotrypsin-related function network includes many distributed activities in ATP-dependent proteases, ATP-dependent chaperone proteases and chaperonins, protein export, and control of the misfolding, refolding, proper assembly of polypeptides, which are critical for digestion and stress-induced, heat shock or hyperosmotic damages systems.

Conclusion

The present research computationally evaluated the potential impact of the proregions from insect zymogens to inhibit the function of the *S. exigua* digestive chymotrypsin as a potent agent for pest management.

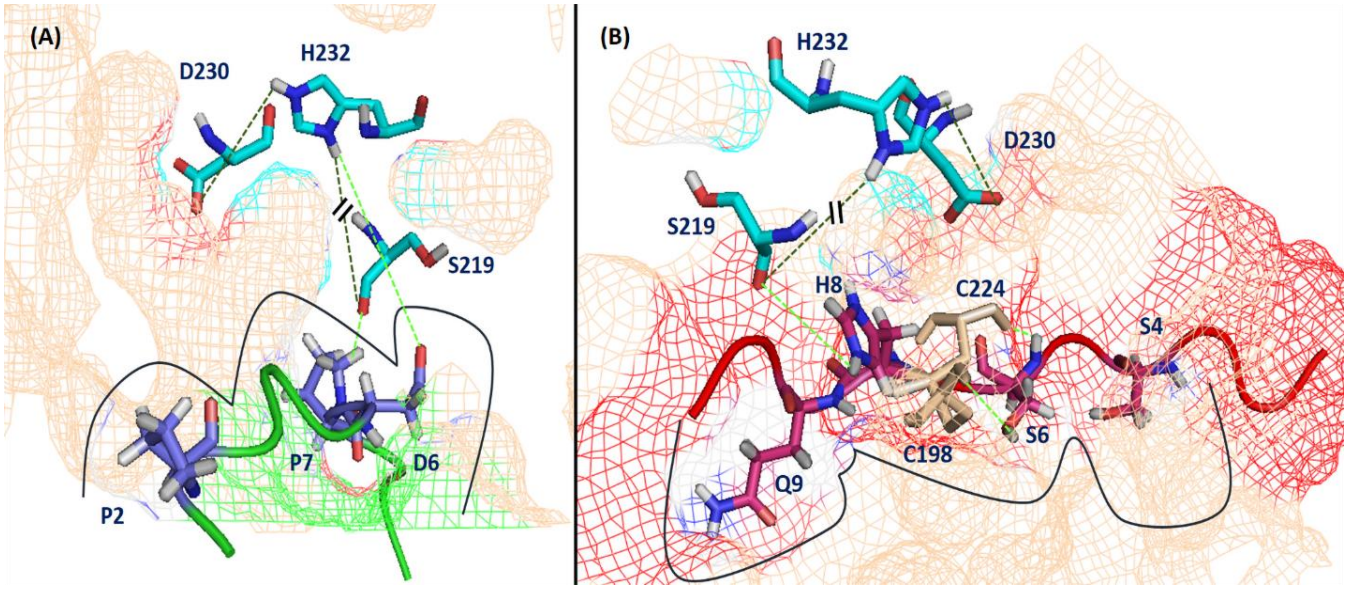

Figure 5. Peptide-1 (A) and peptide-5 (B) mechanism of catalytic function disruption of *S. exigua* chymotrypsin. The dark green dash lines indicate chymotrypsin catalytic triad hydrogen bonds and the light green dash lines are peptide-induced hydrogen bonds. In both representations, the internal S219 and H232 hydrogen bond is disrupted in the chymotrypsin catalytic cleft.

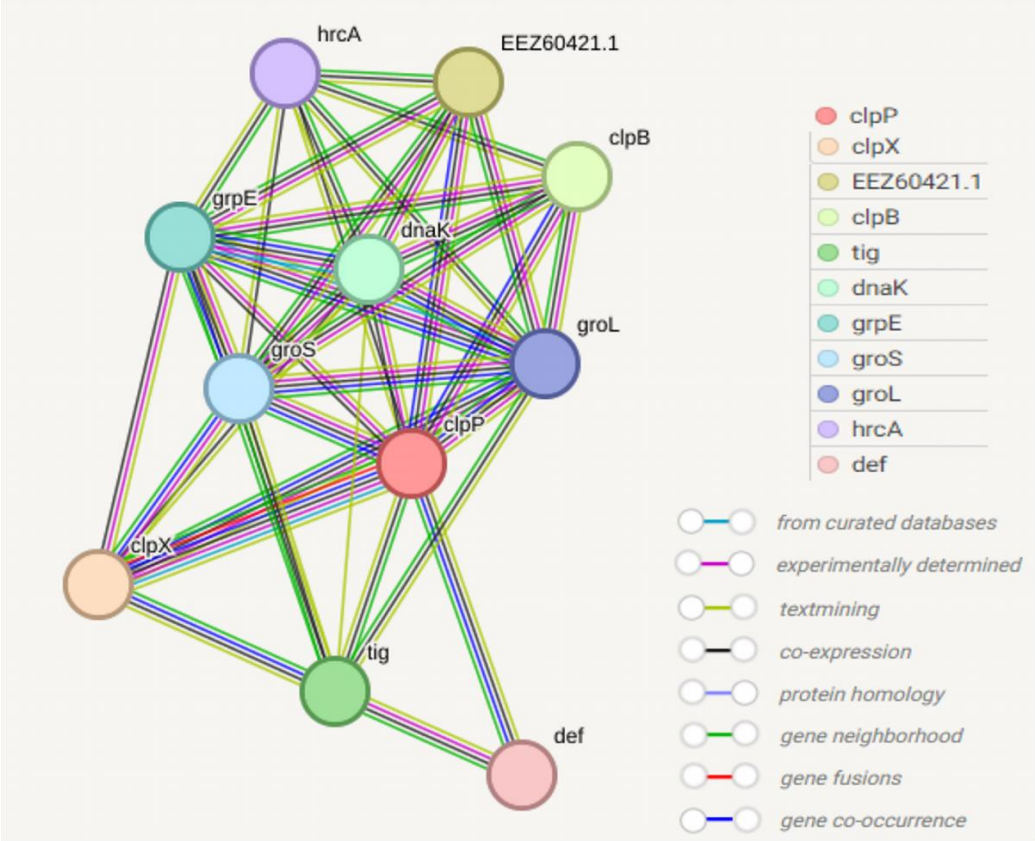

Figure 6. Protein-protein interaction network of midgut chymotrypsin detected through STRING. The red node (clpP protein) represented chymotrypsin and other nodes represented its predicted functional partners on the right side. The minimum interaction score was set at medium confidence (0.4). The interacting line meaning is depicted on the right down site.

The study also discovered the molecular mechanisms and binding energies involved in interactions between screened peptides and *S. exigua* chymotrypsin. Furthermore, the *S. exigua* chymotrypsin structural and physiological properties were also reported in addition to active site identification and protein-protein network interactions. The assessment of the interactions between the pro-peptides and the enzyme confirmed the potency of the selected peptides for inhibiting the enzyme. Data from molecular simulation techniques emphasized that screened peptides are promising strategies for dealing with pest infestations and crop losses with fewer side effects. However, further *in vitro* and *in vivo* validation is needed for the efficiency of the best-scoring inhibitor peptides.

Acknowledgments

This research was received financial support by the Shahid Chamran University of Ahvaz, Ahvaz, Iran (Grant No. SCU.AP1402.39134), which is greatly appreciated.

References

Baker, D., Shiau, A. K., & Agard, D. A. (1993). The role of pro regions in protein folding. *Current opinion in cell biology*, *5*(6), 966-970. https://doi.org/10.1016/0955-0674(93)90078-5

Brewer, M. J., Trumble, J. T., Alvarado-Rodriguez, B., & Chaney, W. E. (1990). Beet armyworm (Lepidoptera: Noctuidae) adult and larval susceptibility to three insecticides in managed habitats and relationship to laboratory selection for resistance. *Journal of Economic Entomology*, *83*(6), 2136-2146. https://doi.org/10.1093/jee/83.6.2136

Franco, O. L., Rigden, D. J., Melo, F. R., & Grossi-de-Sá, M. F. (2002). Plant α-amylase inhibitors and their interaction with insect α-amylases: Structure, function and potential for crop protection. *European journal of biochemistry*, *269*(2), 397-412. https://doi.org/10.1046/j.0014-2956.2001.02656.x

Fu, X., Feng, H., Liu, Z., & Wu, K. (2017). Trans-regional migration of the beet armyworm, *Spodoptera exigua* (Lepidoptera: Noctuidae), in North-East Asia. *PLoS One*, *12*(8), e0183582. https://doi.org/10.1371/journal.pone.0183582

Greenberg, S. M., Sappington, T. W., Legaspi, B. C., Liu, T. X., & Setamou, M. (2001). Feeding and life history of *Spodoptera exigua* (Lepidoptera: Noctuidae) on different host plants. *Annals of the Entomological Society of America*, *94*(4), 566-575. https://doi.org/10.1603/0013-8746(2001)094[0566:FALHOS]2.0.CO;2

Hemmati, S. A. (2021). Structural, functional, and phylogenetic studies of chymotrypsin enzyme genes in insects: a bioinformatics approach. *Plant Protection (Scientific Journal of Agriculture)*, *43*(3), 43-60. https://doi.org/10.22055/ppr.2020.16417

Hemmati, S. A., & Karam Kiani, N. (2020). Evaluation of the inhibitory potential of pro-peptide region as the inhibitor of the digestive chymotrypsin of cotton bollworm, *Helicoverpa armigera* (Lepidoptera: Noctuidae), based on in silico studies. *Journal of Entomological Society of Iran*, *40*(3), 237-253. https://doi.org/10.22117/jesi.2020.342422.1371

Hemmati, S. A., Karam Kiani, N., Serrão, J. E., & Jitonnom, J. (2021a). Inhibitory potential of a designed peptide inhibitor based on zymogen structure of trypsin from *Spodoptera frugiperda*: in silico insights. *International Journal of Peptide Research and Therapeutics*, *27*, 1677-1687. https://doi.org/10.1007/s10989-021-10200-4

Hemmati, S. A., Sajedi, R. H., Moharramipour, S., Taghdir, M., Rahmani, H., Etezad, S. M., & Mehrabadi, M. (2017). Biochemical characterization and structural analysis of trypsin from *Plodia interpunctella* midgut: implication of determinants in extremely alkaline pH activity profile. *Physiological Entomology*, *42*(4), 307-318. https://doi.org/10.1111/phen.12196

Hemmati, S. A., Shishehbor, P., & Stelinski, L. L. (2022). Life table parameters and digestive enzyme activity of *Spodoptera littoralis* (Boisd)(Lepidoptera: Noctuidae) on selected legume cultivars. *Insects*, *13*(7), 661. https://doi.org/10.3390/insects13070661

Hemmati, S. A., Takalloo, Z., Taghdir, M., Mehrabadi, M., Balalaei, S., Moharramipour, S., & Sajedi, R. H. (2021b). The trypsin inhibitor pro-peptide induces toxic effects in Indianmeal moth, *Plodia interpunctella*. *Pesticide Biochemistry and Physiology*, *171*, 104730. https://doi.org/10.1016/j.pestbp.2020.104730

Huang, J. M., Zhao, Y. X., Sun, H., Ni, H., Liu, C., Wang, X., Gao, C. H., & Wu, S. F. (2021). Monitoring and mechanisms of insecticide resistance in *Spodoptera exigua* (Lepidoptera: Noctuidae), with special reference to diamides. *Pesticide Biochemistry and Physiology*, *174*, 104831. https://doi.org/10.1016/j.pestbp.2021.104831

Jitonnom, J., Lomthaisong, K., & Lee, V. S. (2012). Computational design of peptide inhibitor based on modifications of proregion from *Plutella xylostella* midgut trypsin. *Chemical biology & drug design*, *79*(4), 583-593. https://doi.org/10.1111/j.1747-0285.2011.01312.x

Kumari, R., Kumar, R., Open Source Drug Discovery Consortium, & Lynn, A. (2014). *g_mmpbsa*-A GROMACS tool for high-throughput MM-PBSA calculations. *Journal of chemical information and modeling*, *54*(7), 1951-1962. https://pubs.acs.org/doi/10.1021/ci500020m

Macindoe, G., Mavridis, L., Venkatraman, V., Devignes, M. D., & Ritchie, D. W. (2010). HexServer: an FFT-based protein docking server powered by graphics processors. *Nucleic acids research*, *38*(suppl_2), W445-W449. https://doi.org/10.1093/nar/gkq311

Omkar, O. (2016). *Ecofriendly Pest Management for Food Security*. Elsevier Ltd. https://shop.elsevier.com/books/ecofriendly-pest-management-for-food-security/omkar/978-0-12-803265-7

Pereira, M. E., Dörr, F. A., Peixoto, N. C., Lima-Garcia, J. F., Dörr, F., & Brito, G. G. (2005). Perspectives of digestive pest control with proteinase inhibitors that mainly affect the trypsin-like activity of *Anticarsia gemmatalis* Hübner (Lepidoptera: Noctuidae). *Brazilian Journal of Medical and Biological Research*, *38*, 1633-1641. https://doi.org/10.1590/S0100-879X2005001100010

Robinson, G. S., Ackery, P. R., Kitching, I. J., Beccaloni, G. W., & Hernández, L. M. (2010). HOSTS-a Database of the World's Lepidopteran Hostplants. *Natural History Museum, London*, *11*(03), 2017.

Silva, F. B., Monteiro, A. C. S., Del Sarto, R. P., Marra, B. M., Dias, S. C., Figueira, E. L. Z., Oliveira, G. R., Rocha, T. L., Souza, D. S. L., da Silva, M. C. M., Franco, O. L., & Grossi-de-Sa, M. F. (2007). Proregion of *Acanthoscelides obtectus* cysteine proteinase: A novel peptide with enhanced selectivity toward endogenous enzymes. *peptides*, *28*(6), 1292-1298. https://doi.org/10.1016/j.peptides.2007.03.020

Smits, P. H., Van Velden, M. C., Van de Vrie, M., & Vlak, J. M. (1987). Feeding and dispersion of *Spodoptera exigua* larvae and its relevance for control with a nuclear polyhedrosis virus. *Entomologia Experimentalis et Applicata*, *43*(1), 67-72. https://doi.org/10.1111/j.1570-7458.1987.tb02204.x

Taylor, M. A., & Lee, M. J. (1997). Trypsin isolated from the midgut of the tobacco hornworm, *Manduca sexta*, is inhibited by synthetic pro-peptidesin vitro. *Biochemical and biophysical research communications*, *235*(3), 606-609. https://doi.org/10.1006/bbrc.1997.6839

Van Der Spoel, D., Lindahl, E., Hess, B., Groenhof, G., Mark, A. E., & Berendsen, H. J. (2005). GROMACS: fast, flexible, and free. *Journal of computational chemistry*, *26*(16), 1701-1718. https://doi.org/10.1002/jcc.20291

Visal, S., Taylor, M. A., & Michaud, D. (1998). The proregion of papaya proteinase IV inhibits Colorado potato beetle digestive cysteine proteinases. *FEBS letters*, *434*(3), 401-405. https://doi.org/10.1016/S0014-5793(98)01018-7

Wheeler, W. B. (Ed.). (2002). *Pesticides in Agriculture and the Environment*. CRC Press.

Zeng, J., Kong, X., Dong, Z., Wu, J., & Li, Y. (2019). Effects of five different host plants on the midgut protease activities of the larva in *Spodoptera exigua*. *Journal of Environmental Entomology*, *41*(1), 42-49. https://www.cabdirect.org/cabdirect/abstract/20193268192

گیاه‌پزشکی (مجله علمی کشاورزی)
جلد ٤٦، شماره ۳، پاییز ۱٤۰۲

10.22055/ppr.2024.46044.1733

بررسی محاسباتی پروپپتیدهای زیموژن های حشرات به عنوان مهارکننده های تقلیدی برای کیموتریپسین گوارشی کرم برگ‌خوار چغندرقند، *Spodoptera exigua*

سید علی همتی [۱*] و خدیجه پورآقاجان [۲و۳]

۱- **نویسنده مسوول**: دانشیار، گروه گیاه‌پزشکی، دانشکده کشاورزی، دانشگاه شهید چمران اهواز، اهواز، ایران (sa.hemmati@scu.ac.ir)

۲- محقق، گروه علوم، شرکت ویتابیوتکس، شعبه ایران، تهران، ایران

۳- دکتری تخصصی، آزمایشگاه بیوانفورماتیک، گروه زیست‌شناسی، دانشکده علوم، دانشگاه رازی، کرمانشاه، ایران

تاریخ دریافت: ۱۴۰۲/۱۱/۱۵ تاریخ پذیرش: ۱۴۰۲/۱۲/۲۶

چکیده

یکی از مخرب‌ترین آفات محصولات کشاورزی، *Spodoptera exigua* (Hübner) می‌باشد که بطور معمول با آفت‌کش‌های شیمیایی، که دارای اثرات مخربی می‌باشند، کنترل می‌شود. از این رو، بررسی راهبردهای جدید کنترل آفات بسیار مهم بنظر می‌رسد. یکی از این راهبردها، استفاده از مهارکننده‌های پروتئاز گوارشی آفت می‌باشد. بسیاری از پروتئازها به صورت زیموژن با نواحی پروپپتید در انتهای آمینی تولید می‌شوند که می‌توانند به عنوان چاپرون‌های درون مولکولی و مهارکننده‌های پروتئازی نقش ایفا نمایند. در مطالعه حاضر، هدف شناسایی ساختار و خواص کیموتریپسین *S. exigua* از طریق ابزارهای محاسباتی و همچنین بررسی بازدارنده‌های پپتیدی مشتق شده از ناحیه پروپپتیدی زیموژن‌ها که می‌توانند به عنوان مهارکننده‌های تقلیدی برای کیموتریپسین آفت مورد استفاده قرار گیرند، انجام شد. بنابراین، چندین ابزار بیوانفورماتیک برای بررسی خواص فیزیکوشیمیایی، ساختارهای ثانویه و توپولوژی کیموتریپسین از *S. exigua* مورد استفاده قرار گرفت. مدل‌سازی مولکولی همسانی با استفاده از SWISS-MODEL انجام شد و اعتبار مدل پیش‌بینی‌شده توسط برنامه‌های مختلف سنجیده شد. مطالعات اتصال مولکولی بین پنج مهارکننده پروتئاز مشتق از گونه‌های همولوگ و مدل پیش‌بینی‌شده و به دنبال آن شبیه‌سازی دینامیک مولکولی همراه با محاسبات ناحیه سطحی پواسون-بولتزمن (MMPBSA) مکانیک مولکولی انجام شد. آنالیز برهمکنش‌های پپتید/آنزیم، ظرفیت آنتاگونیستی برای دو پپتید را نشان داد. بعلاوه، بررسی شبکه برهمکنش پروتئین-پروتئین نشان داد که کیموتریپسین از *S. exigua* با یازده پروتئین دیگر در یک امتیاز اطمینان بالا تعامل داشت. تجزیه و تحلیل جایگاه فعال نشان داد که S219، D230، و H232 به عنوان باقی مانده های کاتالیزوری عمل می کنند. یافته‌های این پژوهش، نقش کلیدی روش‌های محاسباتی در طراحی و انتخاب پپتیدهای مهارکننده با عملکرد بسیار اختصاصی را نشان می‌دهد که می‌تواند به عنوان نقطه عطفی برای طراحی حشره‌کش‌های مورد استفاده در کنترل *S. exigua* در نظر گرفته شود.

کلیدواژه‌ها: Spodoptera exigua، کیموتریپسین، پروپپتید، پپتید مهاری، مدیریت آفت

دبیر تخصصی: دکتر سهیلا محمدی

Citation: Hemmati, S. A. & Pouraghajan, Kh. (2024). In silico investigation of pro-peptides from insect zymogens as mimetic inhibitors for digestive chymotrypsin of beet armyworm, *Spodoptera exigua*. *Plant Protection (Scientific Journal of Agriculture)*, *46*(3), 127-142. https://doi.org/ 10.22055/ppr.2024.46044.1733.